SINTEZA, CARACTERIZAREA ȘI EVALUAREA COMPORTAMENTULUI TERMIC A UNEI STICLE DE FOSFAT DE FIER DESTINATĂ IMOBILIZĂRII DEȘEURILOR NUCLEARE
SYNTHESIS, CHARACTERIZATION AND THERMAL BEHAVIOR ASSESSMENT OF AN IRON PHOSPHATE GLASS DEDICATED FOR NUCLEAR WASTE CONFINEMENT

A. DJERIDI[1] * , N. KAMEL[2], A. BENMOUNAH[1], D. MOUDIR[2], S. KAMARIZ[2], Y. MOUHEB[2]

[1] *Research Unit for Materials, Processes and Environment, University M' Hamed Bouguara of Boumerdes, Boumerdes, 35000, Algeria.*
[2] *Algiers Nuclear Research Centre, Division of Nuclear Techniques, 2. Bd Frantz Fanon, P.O. Box: 399, Alger-RP, Algiers, Algeria.*

An iron phosphate glass in the system 25 wt.% Fe_2O_3- 57 wt.% P_2O_5 - 8 wt.% B_2O_3 - 8 wt.% Na_2O - 2 wt.% As_2O_3 was synthesized by a double melting /casting method at 1100°C. Fe/P is atomic weight ratio is fixed to 0.67. 20 wt.% of simulated nuclear wastes were successfully immobilized in the glass bulk. Both density and molar volume, measured for both pure and waste loaded glasses, are representative values of phosphate glasses. X-ray diffraction analysis confirmed the amorphous feature of both glasses, and scanning electron microscopy allows the microstructure observations. The glass transition temperature (T_g), the crystallization (T_c) and melting (T_m) temperatures are measured by DTA analysis. T_g = 623 and 580°C; T_c= 766 and 679 °C and T_m=933 and 929 °C; for the pure and RW loaded glasses, respectively. Hruby ($K_H =(T_c - T_g)/(T_m - T_c)$), Weinberg ($K_W =(T_c - T_g)/T_m$) and Lu/Liu ($K_{LL} = T_c/(T_g + T_m)$) criteria were used for the evaluation of glass stability of both pure and radioactive waste loaded glasses. Although the values are lower for the radioactive waste loaded glass compared to those for the pure glass, and thus, the no loaded glass is more stable than the radioactive waste loaded one. The calculated criteria remain in an acceptable interval between 0.11-0.86, suggesting that the glass stability is not altered by the addition of 20 wt.% of simulated radioactive waste. The glass forming ability (GFA) is assessed by $\Delta T_{xg} =(T_x − T_g)$, ω_2, α, β, γ_m, and ε criteria. The calculated criteria allow valuable conclusions on the good thermal behavior of the radioactive waste loaded phosphate glass.

Keywords: Iron phosphate glass, Thermal stability, Glass forming ability, Radioactive waste, DTA, XRD, SEM.

1. Introduction

Phosphate glasses are interesting materials from both scientific and technological points of view, due to their specific physical properties such as low melting temperatures (less then 1000°C) and glass transition temperatures over 500°C [1-9], high thermal expansions coefficients [4-9], high ultra-violet transmission, high electrical conductivity and compositional flexibility [7−9]. Therefore, they are useful for a wide range of applications such as laser hosts [10], biomedical devices [11], solid electrolytes [12], and nuclear waste immobilization materials [13].

R.K. Brow et al. [7] published a pertinent review on phosphate glasses up to the 2000 year.

However, phosphate glasses present a poor chemical durability which makes them unsuitable for practical applications [14-16], especially in the field of nuclear waste immobilization. It was reported [16-22] that the introduction in their structure of oxides such as SnO, PbO, ZnO, Cr_2O_3 and Fe_2O_3, results in the formation of Sn-O-P, Pb-O-P, Zn-O-P, P-O-Cr and P-O-Fe bonds, and leads to improvement in the chemical durability of such modified phosphate glasses.

The physical and chemical properties of phosphate glasses can be optimized by controlling the melting conditions and chemical composition. The poor chemical durability of phosphate glasses can be significantly enhanced by the addition of Fe_2O_3 [23−25]. The resulting iron phosphate glasses (IPG) are of great interest for several technological and biological applications [26,27].

IPG materials are considered as alternative glasses for the immobilization of High Level Wastes (HLW) due to their sealing features, namely their good glass forming ability and very high waste loading, a favorable chemical stability [23,28], and low melting temperatures, generally between 950 and 1100°C [29].

Among the various chemical compositions of IPG, the glass with Fe/P atomic weight ratio approaching 0.67 seems to be chemically the most durable one [30].

The structure of the IPG glass is based on corner-sharing PO_4 tetrahedra which form chains, rings or isolated PO_4 groups. With the addition of Fe_2O_3 to the glass, the P−O−P bonds are replaced by P−O−Fe^{2+} and/or P−O−Fe^{3+} bonds, which are more chemically durable [25,33]. In IPG glass, iron commonly exists in two valence states: Fe^{2+} and

---

Fe^{3+} and ($Fe^{2+} \Leftrightarrow Fe^{3+}$) equilibrium depends upon the melting atmosphere and the batch composition [32,33].

The purpose of this study is to synthesize an IPG, in the following glass system: 25 wt.% Fe_2O_3- 57 wt.% P_2O_5 - 8 wt.% B_2O_3 - 8 wt.% Na_2O - 2 wt.% As_2O_3, by a double melting method, at 1100°C. Fe/P is atomic weight ratio is fixed to 0.67. The glass is loaded by a Ce-rich complex nuclear waste mixture, containing over 25 elements. The radioactive waste (RW) chemical composition is inspired by both this of HLW originate from fast reactor fuel reprocessing [34], and the HLW generated from spent electrolyte used for pyrochemical reprocessing in Japan [35,36]. The glass density is measured and the molar volume calculated. Both the pure and RW loaded glasses are characterized by X-ray diffraction, Scanning Electronic Microscopy, and Differential Thermal Analysis methods. The glass stability was assessed by Hruby, Weinberg and Lu/Liu criteria.

2. Experimental

2.1. Preparation of glass samples

The glasses are prepared using the method of two melting/casting steps.

The following commercial reagents are employed: Al_2O_3 (Fluka, 98%), As_2O_3 (Fluka, 99.5), B_2O_3 (Fluka, Purity ≥ 99%), CaF_2 (Merck), CaO (Merck, ≥ 97%), CdO (Fluka, ≥98%), CeO_2 (Aldrich, 99.999%), Cr_2O_3 (Reachim), Fe_2O_3 (Merck, ≥ 99%), K_2O (Merck, ≥ 99%), MgO (Fluka, ≥ 97%), MnO_2 (Merck), MoO_3 (Merck, ≥ 99.5%), Na_2O (99.5), Nd_2O_3 (Fluka, ≥ 99.9%), P_2O_5 (Merck, Purity ≥ 98%), Pr_6O_{11} (Merck, ≥ 99%), Rb_2O (Merck, 99%), SnO_2 (Merck, 99.5%), TiO_2 (Merck, ≥ 99%), U_3O_8 (Prolabo), Y_2O_3 (Merck, ≥ 99%), ZnO (Merck, 99%) and ZrO_2 (Aldrich, 99%).

The Rare earth elements' (REE) oxides are dried over night at 1 000 °C, and the other oxides at 400 °C, for the same time duration. This step ensures a good homogeneity of the products, and confers them isotropic properties.

BaO, La_2O_3 and NiO are prepared by calcination at 450°C of $BaNO_3$ (Fluka, 99.6%), $La(NO_3)_3 \cdot 6H_2O$ (Fluka, 99.99%), and $Ni(NO_3)_2 \cdot 6H_2O$ (Fluka, 99.6%), respectively. Ag_2O is prepared by calcination of $Ag(NO_3)$ (Sigma Aldrich, 99.9%) at 120 °C for 4 h [37], and SrO by calcination of $Sr(NO_3)$ (Biochim, ≥ 98%) at 580°C for 3 h 30 min [37]. CoO is the calcination product at 250°C of $Co(NO_3).6H_2O$ (Merck, ≥ 99%) [38], and Gd_2O_3, the calcination product at 465°C of $Gd(NO_3)_3.6H_2O$ (Aldrich, 99.99%) [39]. Cs_2O is prepared by calcination of $CsNO_3$ (Biochim, 99.5%) at 600 °C for 3 h 30 min [37], and Nd_2O_3 by calcination of $Nd(NO_3)_3.6H_2O$ (Labosi, 99.5%) at 520°C for 2 h [40]. All the as prepared oxides are analyzed by X-ray fluorescence spectrometry (XRF) and X-ray diffraction (XRD) to confirm their chemical composition. The whole of reagents are milled in a Retsch Gmbh 5657 automatic agath mortar, until the particles grains sizes becomes lower than 20 μm.

The phosphate glass (PG) is prepared by weighing and mixing thoroughly the different reagents according to the chemical composition of Table 1. Fe/P atomic weight ratio is fixed to 0.67. P_2O_5 is combined with the other oxides due to its hygroscopic nature. The mixture is homogenized in an Automatic Sieve Shaker D403 during 5 h, to achieve a good particles' dispersion. The powders mixture are melted in high purity alumina crucibles, in a high temperature HF1800 Carbolite furnace at a temperature of 1100°C during 2 h, with a heating step of 10°C/min. The melted glasses are poured in water, grinded in a manual heavy alloy mortar; protected with a cotton fiber tissue, to avoid glasses contamination. Then, they are milled in a Retsch Gmbh 5657 automatic agath mortar. The grinded glasses are re-melted with the same heating cycle, at 1100°C for 1 h, in order to insure homogeneity in glasses microstructures.

Table 1

Chemical composition of PG and PG+RW glasses

Oxide	PG (wt.%)	RW (wt.%)	PG+RW (wt.%)
Ag_2O		0.256	0.051
Al_2O_3		2.562	0.512
As_2O_3	2.000	0.000	1.600
B_2O_3	8.000	0.000	6.400
BaO		1.367	0.273
CaF_2		0.854	0.171
CaO		3.246	0.649
CdO		0.085	0.017
CeO_2		49.539	9.908
CoO		0.342	0.068
Cr_2O_3		0.512	0.103
Cs_2O		2.904	0.581
Fe_2O_3	25.000	11.958	22.392
Gd_2O_3		0.342	0.068
K_2O		0.512	0.102
La_2O_3		0.683	0.137
MgO		6.833	1.367
MnO_2		0.051	0.010
MoO3		5.125	1.025
Na_2O	8.000	0.000	6.400
Nd_2O_3		3.075	0.615
NiO		0.854	0.171
P_2O_5	57.000	0.000	45.600
Pr_6O_{11}		0.854	0.171
Rb_2O		0.171	0.034
SnO_2		0.137	0.027
SrO		0.342	0.068
TiO_2		0.068	0.014
U_3O_8		0.495	0.099
Y_2O_3		3.758	0.752
ZnO		0.854	0.171
ZrO_2		2.221	0.444
Total (wt.%)	100.000	100.000	100.000

The PG loaded by a Ce-rich complex nuclear waste mixture (PG+RW) is prepared similarly by mixing 80 wt.% of PG with 20 wt.% of the radioactive waste (RW) mixture. The chemical composition of this last mixture is given in Table 1. Fe/P is atomic weight ratio is fixed to 0.67.

A batch of 100 g of the powder mixture is melted in alumina crucibles at 1050°C during 2 h, with a heating step of 10°C/min, in the same furnace. The melted glasses are poured in water, and milled in the same automatic agath mortar, used for the PG. The grinded glasses are re-melted, at 1050°C for 1 h. The melts are casted in cylindrical molds and annealed at 475°C for 1 h 30 min to eliminate internal stress, and cooled to room temperature, with a cooling rate of 1°C/min.

In order to perform characterizations measurements, the cylindrical pellets of 10 mm diameter, are divided in two samples groups. The first pellets group is cut in fine slices of 1 mm, and the second one is ground in order to obtain the powder form.

2.2. Glasses Characterization

The glasses density (d) is measured by Archimedes method using a Kern hydrostatic balance, at "Research Unit for Materials, Processes and Environment (URMPE), of Boumerdes' M'Hamed Bougara University. Water is used as immersion liquid. The results are mean values of three repeated measures.

The volume filled by one mole of glass, V_m, is calculated using the number 1 mathematical formula:

$$V_m = \frac{\sum_i c_i M_i}{d} \qquad (1)$$

Where c_i is the i oxide molar concentration; M_i its molar weight; and d the experimental density.

The glass oxygen molar volume, V_m^O is the volume filled by one mole of oxygen. It is calculated using the number 2 mathematical formula:

$$V_m^o = \frac{\sum_i c_i M_i}{d \sum_i n_i c_i} \qquad (2)$$

Where n_i is the i oxide oxygen stoichiometry [41].

X-ray diffraction analysis is carried out with a Philips X'Pert PRO spectrometer, operating at CuKα1 wavelength (λKα1 = 0.15406 nm). Spectra are recorded from 2 θ = 10 to 90° at a scanning rate of 0.02°/min. V=45 kV and I=40 mA. Phases' identification is performed using a Philips X'Pert plus 2004 software, using COD data base [42].

The glasses microstructure is revealed by Scanning Electron Microscopy (SEM) analysis on transversal sections of both pure and RW loaded glasses, using a Philips XL30 microscope.

In order to identify the glass transition (T_g) crystallization (T_c) and melting (T_m) temperatures, of both pure and RW glasses, we performed

Differential thermal analyses (DTA) with a NETZSCH STA 409PC/PG thermal analyzer, in the laboratory of URMPE. The analyses conditions are: a heating rate of 5 °C/min from 20 to 1200°C. The temperatures uncertainty is ± 1°.

In order to study the glass thermal characteristics, we assessed both the glass forming ability (GFA) and the glass stability (GS).

GS expresses the glass' resistance to crystallization during re-heating [43]. GS can be estimated from T_g, T_c and T_m values, by Hruby (K_H), Weinberg (K_W) and Lu/Liu (K_{LL}) criteria [44-46].

$$K_H = (T_c - T_g)/(T_m - T_c) \qquad (3)$$
$$K_W = (T_c - T_g)/T_m \qquad (4)$$
$$K_{LL} = T_c/(T_g + T_m) \qquad (5)$$

GFA gives information on a melt crystallization resistance during cooling [43]. The GFA criterion is based on the stability of a super-cooled liquid against crystallization.

The parameters used for GFA assessment are ΔT_{xg} criterion, ω_2, α, β, γ_m, and ε. The criteria are defined by the mathematical formulas 6, 7, 8, 9, 10 and 11, respectively [47].
The higher is ΔT_{xg}, the better is the glass GFA.

$$\Delta T_{cg} = T_c - T_g \qquad (6)$$
$$\alpha = \frac{T_c}{T_m} \qquad (7)$$
$$\beta = \frac{T_g T_c}{(T_m - T_c)^2} \qquad (8)$$
$$\gamma_m = \frac{2T_c - T_g}{T_m} \qquad (9)$$
$$\varepsilon = \left[\frac{\Delta T_{cg}}{T_c}\right] + \left[\frac{T_g}{T_m}\right] \qquad (10)$$
$$\omega_2 = \left[\frac{T_g}{2T_c - T_g}\right] - \left[\frac{T_g}{T_m}\right] \qquad (11)$$

3. Results and discussion

3.1. Density and molar volume measurements

Both Archimedes densities and molar volumes of the PG and PG+RW glasses are given in Table 2.

Table 2

Archimedes' densities and molar volumes of both PG and PG+RW glasses.

Glasses	d (g/cm³)	V_m (cm³ ·mol⁻¹)	V_m^O (cm³ ·mol⁻¹)
PG	2.8877	42.635	11.614
PG+RW	3.1779	39.122	11.790

The density of PG+RW waste form is 3.178 g/cm³, whereas that of PG is 2.888 g/cm³. The PG+RW waste form glass molar volume is 39.122 cm³/mol, and that of PG, 42.635 cm³/mol. The effect of waste loading in the matrix is traduced by a rise in the glass density, and a decrease of molar volume.

A. Djeridi, N. Kamel, A. Benmounah, D. Moudir, S. Kamariz, Y. Mouheb / Sinteza, caracterizarea și evaluarea comportamentului
termic a unei sticle de fosfat de fier destinată imobilizării deșeurilor nucleare
445

3.2. Phases identification and microstructure observations

The XRD spectra are given in Figure 1. The phases' identification, performed using a Philips X'Pert plus 2004 software, using COD database [42], confirms the amorphous structure of the PG glass, and reveals minor phases of $Rb_3(BP_2)$, identified to the JCPDS standard N°01-085-0183, and $Na_2Al_2As_3$, identified to the JCPDS standard N°01-084-2302.

Typical SEM micrographs of the pure and RW loaded glasses are depicted on Figure 2.

The micrographs, taken in the bulk of the materials, on fine slices, confirm the homogeneity of the PG glass, and show small crystallites on the surface of the PG+RW glass. The square crystallites correspond to $Rb_3(BP_2)$ phase, and the long ones to $Na_2Al_2As_3$ phase.
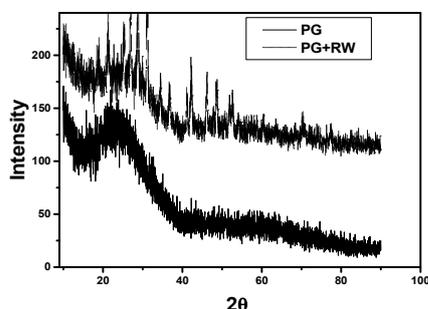

Fig.2 – Typical SEM micrographs of PG (a) and PG+RW (b) glasses.

Fig.1 - XRD spectra of the PG and PG+RW glasses.

3.3. Thermal stability

T_g, T_c and T_m glasses temperatures are measured for PG and PG+RW glasses, for comparison purposes, in order to elucidate the effect of RW loading during the glass formation. DTA diagrams are depicted in Figure 3. The allotropic transformations temperatures are given in Table 3.

T_g value of the pure glass is of 623.48°C and decreases to 580.04°C when loading the glass with the complex oxides mixture of RW. However, this value is acceptable since it is over the waste package temperature during storage (550°C). Both the crystallization and melting temperatures decreases also when loading the glass with the RW powder mixture: one can remark a T_c
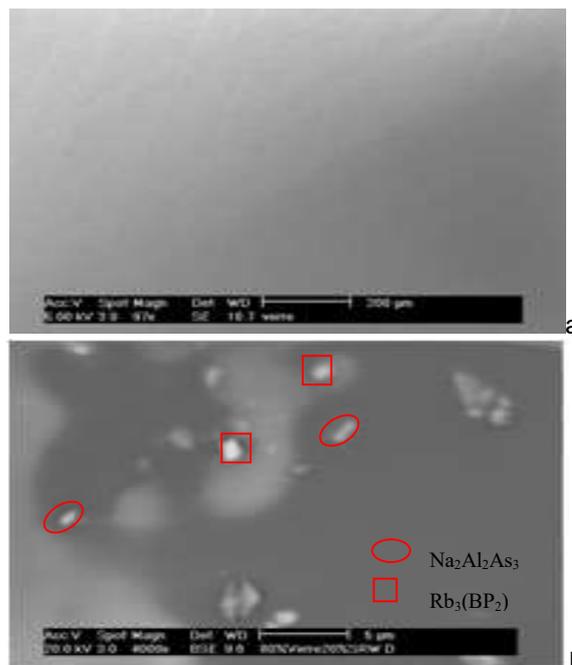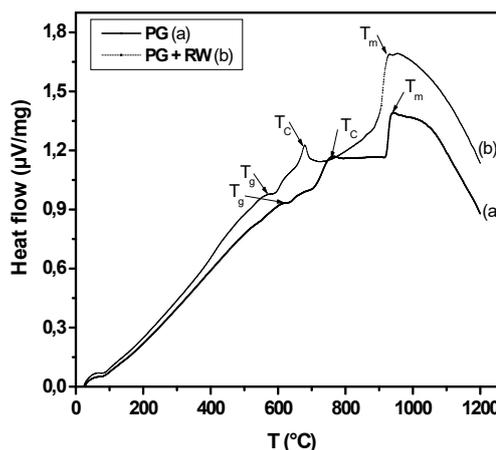

Fig.3 - DTA diagrams of both the PG (a) and PG+RW (b) glasses.

decrease of 87°C from 766.34 to 679.26°C, from the pure to the RW loaded glass; and a little decrease of 3°C of T_m from 932.75 to 929.43°C.

Table 3

Allotropic transformation temperatures and GS criteria of both PG and PG+RW glasses

Glasses	T_g (°C)	T_c(°C)	T_m(°C)	$K_H \pm 10^{-3}$	$K_W \pm 10^{-3}$	$K_{LL} \pm 10^{-3}$
PG	623.48	766.34	932.75	0.86	0.15	0.49
PG+RW	580.04	679.26	929.43	0.41	0.11	0.45
PG [34]	509.85	694.85	924.85	0.80	0.15	0.49
PG loaded by simulated fast reactor waste [34]	511.85	676.85	917.85	0.69	0.15	0.48
PG [48]	528-579	747-872	---	---	---	---
PG [49]	526-529	625-627	---	---	---	---
PG [36]	488-522	---	---	---	---	---

S. Li et al. [48] studied the influence of the content in MgO, CaO, SrO on the glass stability for the following glass chemical composition: (100-x)($0.6P_2O_5–0.4Fe_2O_3$)-xRO (RO=MgO, CaO, SrO, x=5, 10, 15, 20 mol.%) and found that both T_g and T_c temperatures increases with MgO and CaO contents (Tg varies from 528 to 579°C, and T_c from 747 to 876 °C) contrary to the glasses where SrO content rises. These last glasses slump dramatically, and their thermal stability is compromised as well.

Q. Liao et al. [49] synthesize a RW loaded PG glass with Fe_2O contents ranging from 18.6 to 24.6 wt.%. T_g increases slightly from 526 to 529°C, and T_c from 625 to 627°C. These values are lower than the values given in the present paper. They are close to those given by S. Li et al. [48]. This is due to the less content in alkali elements in the present studied glasses.

K. Joseph et al. [34] synthesize a PG glass containing 20 % of simulated fast reactor waste. They found that T_g slightly rises from 509.85 to 511.85 °C and T_c decreases from 694 to 676°C, and T_m from 924 to 917°C. Except for T_c, which is very close to the value found in the present study for PG+RW glass, the other transition temperatures are lower than our values. The similarity in T_c values can be attributed to the similarity in the chemical compositions of both studies.

H. Kofuji et al. [36] studied a PG glass as an alternative waste form for HLW generated from pyrochemical reprocessing. Optimization experiments of glass composition were carried out to investigate the effect of adding transition metal oxides in the glass. T_g temperature varies with the glass chemical composition from 488-522°C.

3.4. Glass stability GS and glass forming ability GFA

Hruby, Weinberg and Lu/Liu criteria are calculated to assess the GS from T_g, T_c and T_m values, for both PG and PG+RW glasses. The calculated criteria are given in Table 3. The calculated values are similar to those of K. Joseph et al. [34] showing the thermal stability of the present studied PG glass.

The larger the values of K_H, K_W and K_{LL} are, the greater would be the GS against crystallization. The reports values in the literature, obtained for many silicate glasses are in the range of 0.14–0.69 [50, 51]. These were calculated using the melting temperature (T_m) during the assessment of GS. Similarity, the criteria values between PG and PG+RW glasses suggest that the glass stability is not altered by the addition of 20 wt.% of RW mixture.

GFA is assessed by ΔT_{xg} criterion, ω_2, α, β, γ_m, and ε parameters. The calculated values are given in Table 4, for both PG and PG+RW. The ΔT_{xg} =(T_x - T_g) criterion, based on the stability of the super-cooled liquid against crystallization, signifies that higher is ΔT_{xg}, better is the GFA. Similar magnitude of ΔT_{xg} values of PG and PG+RW indicates that glass forming ability was not altered by the addition of waste to the glass. The lower are ω_2 values, the better is the glass forming ability of the system. Thus, similar values (magnitude 10^{-2}) of ω_2 also indicates the good GFA of PG+RW glass. Comparable values of the other GFA parameters (α, β, γ_m, and ε) also point out the good GFA characteristics of both PG+RW and PG glasses. The calculated values are similar to those of K. Joseph et al. [34].

Table 4

GFA parameters of both PG and PG+RW

Glass forming criteria	PG	PG+RW	PG [36]	PG+RW [36]
$\Delta T_{cg} = T_c - T_g$	142.86	99.22	185	165
$\alpha = \dfrac{T_c}{T_m}$	0.82	0.73	0.81	0.80
$\beta = \dfrac{T_g T_c}{(T_m - T_c)^2}$	17.25	6.29	14.3	12.8
$\gamma_m = \dfrac{2T_c - T_g}{T_m}$	0.97	0.84	0.96	0.94
$\varepsilon = \left[\dfrac{\Delta T_{cg}}{T_c}\right] + \left[\dfrac{T_g}{T_m}\right]$	0.85	0.77	0.84	0.83
$\omega_2 = \left[\dfrac{T_g}{2T_c - T_g}\right] - \left[\dfrac{T_g}{T_m}\right]$	0.017	0.118	0.025	0.045

4. Conclusion

An iron phosphate glass in the system : 25 wt.% Fe_2O_3- 57 wt.% P_2O_5 - 8 wt.% B_2O_3 - 8 wt.% Na_2O - 2 wt.% As_2O_3 is synthesized by a double melting method at 1100°C, and is loaded by a Ce-rich complex nuclear waste mixture, containing over 25 elements. The effect of waste loading in the matrix is traduced by a rise in the glass density from 2.888 to 3.178 g/cm^3, and a decrease of the molar volume from 39.122 to 42.635 cm^3/mol. Both the PG and PG+RW glasses are characterized by XRD, SEM, and DTA analyses. XRD analysis confirm the amorphous structure of the PG glass, and reveals minor phases of $Rb_3(BP_2)$ and $Na_2Al_2As_3$ phases. SEM analysis allows the microstructure observation of both glasses, and DTA analysis the thermal stability assessment of the as prepared PG glass.

T_g value of the PG glass is of 623.48°C and decreases to 580.04°C when loading the glass with the radioactive waste mixture. However, these values remain acceptable. Both T_c and T_m temperatures decreases when loading the glass with the RW powder mixture. The glasses stability is assessed by Hruby, Weinberg and Lu/Liu criteria. These thermal stability criteria show satisfactory values, in the interval 0.14 – 0.69.

Similar values of ΔT_{xg}, ω_2 criteria of PG and PG+RW glasses indicate that glass forming ability was not altered by the addition of waste to the glass. Comparable values of the other GFA parameters (α, β, γ_m, and ε) also point out the good GFA characteristics of both PG+RW and PG glasses.

REFERENCES

1. L.M. Sanford and P.A. Tick, US Patent 4.314.031, 1982.

2. P.Y. Shih, S.W. Yung and T.S. Chin, Thermal and corrosion behavior of P_2O_5-Na_2O-CuO glasses, J. Non-Cryst. Solids. 1998, **224**(2), 143.

3. P.Y. Shih, S.W. Yung, C.Y. Chen, H.S. Liu and T.S. Chin, The effect of SnO and PbC_{l2} on properties of stannous chlorophosphate glasses, Mater. Chem. Phys, 1997, **50**(1), 63.

4. T.Y. Wei, Y. Hu and L.G. Hwa, Structure and elastic properties of low-temperature sealing phosphate glasses, J. Non-Cryst. Solids. 2001, **288**(1-3), 140.

5. H. Niida, M. Takahashi, T. Uchino and T. Yoko, Preparation and structure of organic-inorganic hybrid precursors for new type low-melting glasses, J. Non-Cryst. Solids. 2002, **306**(3), 292.

6. H.S. Liu, P.Y. Shih and T.S. Chin, Low melting PbO-ZnO-P_2O_5 glasses, Phys. Chem. Glasses. 1996, **37**(6), 227.

7. R.K. Brow, Review: the structure of simple phosphate glasses, J. Non-Cryst. Solids, 2000, **263−264** (3), 1.

8. B.C. Sales, L.A. Boatner, Lead-iron phosphate glass: A stable storage medium for high-level nuclear waste, Science. 1984, **226**(4670), 45.

9. Y. Abe, H. Hosono, Inorganic phosphate materials, Edited by T. Kanazawa. Elsevier, Amsterdam, 1989, p.124.

10. T.T. Fernandez, P. Haro-González, B. Sotillo, M. Hernandez, D. Jaque, P. Fernandez, C. Domingo, J. Siegel, and J. Solis, Ion migration assisted inscription of high refractive index contrast waveguides by femtosecond laser pulses in phosphate glass, Opt. Lett. 2013, **38**(24), 5248.

11. K. Takada, Progress and prospective of solid-state lithium batteries, Acta Mater. 2013, **61**(3), 759.

12. J.K. Christie, R.I. Ainsworth, D. Di Tommaso, and N.H. de Leeuw, Nanoscale chains control the solubility of phosphate glasses for biomedical applications, J. Phys. Chem. B. 2013, **117**(36), 10652.

13. P. Sengupta, A review on immobilization of phosphate containing high level nuclear wastes within glass matrix – Present status and future challenges, J. Hazard. Mater. 2012, **235**, 17.

14. M.R. Reidmeyer, M. Rajaram and D.E. Day, Preparation of phosphorus oxynitride glasses, J. Non-Cryst. Solids. 1986, **85**(1-2), 186.

15. H. Yung, P.Y. Shih, H.S. Liu and T.S. Chin, Nitridation effect on properties of stannous-lead phosphate glasses, J. Am. Ceram. Soc. 1997, **80**(9), 2213.

16. J.L. Rygel and C.G. Pantano, Synthesis and properties of cerium aluminosilicophosphate glasses, J. Non-Cryst. Solids. 2009, **355**(52-54), 2622.

17. P.A. Bingham and R.J. Hand, Sulphate incorporation and glass formation in phosphate systems for nuclear and toxic waste immobilization, Mater. Res. Bull. 2008, **43**(7), 1679.

18. S. Ray, X. Fang, M. Karabulut, G.K. Marasinghe and D.E. Day, Effect of melting temperature and time on iron valence and crystallization of iron phosphate glasses, J. Non-Cryst. Solids. 1999 **249**(1), 1.

19. P.Y. Shih and T.S. Chin, Preparation of lead-free phosphate glasses with low T_g and excellent chemical durability, J. Mater. Sci. Lett. 2001, **20**(19), 1811.

20. C.M. Shaw and J.E. Shelby, Effect of lead compounds on the properties of stannous fluorophosphate glasses, J. Am. Ceram. Soc. 1988, **71**(5), C252.

21. I.W. Donald, Preparation, properties and chemistry of glass- and glass-ceramic-to-metal seals and coatings, J. Mater. Sci. 1993, **28**(11), 2841.

22. A. Šantić and A. Moguš-Milanković, Charge carrier dynamics in materials with disordered structures: A case study of iron phosphate glasses, Croat. Chem. Acta. 2012, **85**(3), 245.

23. D.E. Day, Z. Wu, C.S. Ray and P. Hrma, Chemically durable iron phosphate glass wasteforms, J. Non-Cryst. Solids. 1998, **241**(1), 1.

24. X. Yu, D.E. Day, G.J. Long, R.K. Brow, Properties and structure of sodium-iron phosphate glasses, J. Non-Cryst. Solids. 1997, **215**(1), 21

25. X. Fang, C.S. Ray, A. Moguš-Milanković, D.E. Day, Iron redox equilibrium, structure and properties of iron phosphate glasses, J. Non-Cryst. Solids. 2001, **283**(1-3), 162.

26. B.C. Sales, L.A. Boatner, Radioactive Waste Forms for the Future, Edited by W. Lutze, R.C. Ewing, Elsevier, Amsterdam, 1988, p. 193-213.

27. T. Jermoumi, M. Hafid, N. Niegisch, M. Mennig, A. Sabir, N. Toreis, Properties of $(0.5−x)Zn–xFe_2O_3–0.5P_2O_5$ glasses, Mater. Res. Bull. 2002, **37**(1), 49.

28. K. Joseph, K.V.G. Kutty, P.Chandramohan, P.R. Vasudeva Rao, Studies on the synthesis and characterization of cesium-containing iron phosphate glasses, J. Nucl. Mater. 2009, **384**(3), 262.

29. S. Aqdim, H. El Sayouty, B. Elouad and J.M. Greneche, Chemical durability and structural approach of the lass series $(40-y)$ Na_2O-yFe_2O_3-$5Al_2O_3$-$55P_2O_5$-by IR, X-ray diffraction and Mössbauer spectroscopy, IOP Conference Series: Materials Science and Engineering, 2012, **28**, Article ID: 012003.

30. M. Karabulut, G.K. Marasinghe, C.S. Ray, D.E. Day, O. Ozturk, G.D. Waddill, X-ray photoelectron and Mössbauer spectroscopic studies of iron phosphate glasses containing U, Cs and Bi , J. Non-Cryst. Solids. 1999, **249** (2-3), 106.

31. R.K. Brow, C.M. Arens, X. Yu, D.E. Day, XPS study of iron phosphate glasses, Phys. Chem. Glasses. 1994, **35**(3), 132.

32. C.S. Ray, X. Fang, M. Karabulut, G.K. Matasinghe, D.E. Day, Effect of melting temperature and time on iron valence and crystallization of iron phosphate glasses, J. Non-Cryst. Solids. 1999, **249** (1), 1.

33. G.K. Marasinghe, M. Karabulut, C.S. Ray, D.E. Day, M.G. Shumsky, W.B. Yelon, C.H. Booth, P.G. Allen, D.K. Shuh, Structural features of iron phosphate glasses, J. Non-Cryst. Solids. 1997, **222**, 144.

34. K. Joseph, R. Asuvathraman, R.V. Krishnan, T.R. Ravindran, R. Govindaraj, K.V. Govindan Kutty, P.R. Vasudeva Rao, Iron phosphate glass containing simulated fast reactor waste: Characterization and comparison with pristine iron phosphate glass, J. Nucl. Mater. 2014, **452**(1-3)**, 273.

35. Feasibility study on commercialized fast reactor cycle systems technical study report of phase II - (2) Nuclear fuel cycle systems, JAEA Research Report 2006-043. 2006, 368 (in Japanese).

36. H. Kofuji, T. Yanob, M. Myochina, K. Matsuyama, T. Okita, S. Miyamotoc, Chemical durability of iron-phosphate glass as the high level waste from pyrochemical reprocessing, Proc. Chem. 2012, **7**, 764.

37. K.H. Stern, High temperature properties and decomposition of inorganic salts. Part 3. Nitrates and nitrites, J. Phys. Chem. Ref. Data. 1972, **1**(3), 747.

38. C. Ehrhardt, M. Gjikaj, W. Brockner, Thermal decomposition of cobalt nitrato compounds: Preparation of anhydrous cobalt (II) nitrate and its characterisation by Infrared and Raman spectra, Therm. Acta. 2005, **432**(1), 36.

39. W.W. Wendlandt and J.L. Bear, Thermal decomposition of the heavier rare-earth metal nitrate hydrates, J. Inorg. Nucl. Chem. 1960, **12**(3-4), 276.

40. C.P.J. Van Vuuren and C.A. Strydom, The thermal decomposition of neodymium nitrate, Therm. Acta. 1986, **104**, 293.

41. A. Quintas, O. Majérus, D. Caurant, J.L. Dussossoy, P. Vermaut, Crystallization of a rare earth-rich aluminoborosilicate glass with varying CaO/Na$_2$O ratio, J. Am. Ceram. Soc. 2007, **90**(3), 712.

42. JCPDS data Philips X'Pert high score package, Diffraction data CD-ROM, International Center for Diffraction Data, Newtown Square PA, 2004.

43. J.E. Shelby, Introduction to glass science and technology, second Ed. The Royal Society of Chemistry, RSC, 2005.

44. A. Hruby, Evaluation of glass-forming tendency by means of DTA, Czech. J. Phys. B. 1972, **22**(11), 1187.

45. M.C. Weinberg, Glass-forming ability and glass stability in simple systems, J. Non-Cryst. Solids. 1994, **167**(1-2), 81.

46. Z.P. Lu, C.T. Liu, A new approach to understanding and measuring glass formation in bulk amorphous materials, Intermetallics. 2004, **12**(10-11), 1035.

47. K. Joseph, S. Ghosh, K.V. Govindan Kutty, P.R. Vasudeva Rao, Crystallization kinetics, stability and glass forming ability of iron phosphate and cesium loaded iron phosphate glasses, J. Nucl. Mater. 2012, **426**(1-3), 233.

48. S. Li, H. Liu, F. Wu, Z. Chang, Y. Yue, Effects of alkaline-earth metal oxides on structure and properties of iron phosphate glasses, J. Non-Cryst. Solids. 2016, **434**, 108.

49. Q. Liao, F. Wang, K. Chen, S. Pan, H. Zhu, M. Lu, J. Qin, FTIR spectra and properties of iron borophosphate glasses containing simulated nuclear wastes, J. Mol. Structure. 2015, **1092**, 187.

50. A.A. Cabral, A.A.D. Cardoso, E.D. Zanotto, Glass-forming ability versus stability of silicate glasses, J. Non-Cryst. Solids. 2003, **320**(1-3), 1.

51. S.E. Lin, Y.R. Cheng, W.C.J. Wei, Synthesis and long-term test of borosilicate-based sealing glass for solid oxide fuel cells, J. Eur. Ceram. Soc. 2011, **31**(11), 1975.

****

MANIFESTĂRI ȘTIINȚIFICE / SCIENTIFIC EVENTS

ICG 2018: 20th International Conference on Glass
Prague, Czechia, September 3-4, 2018

The **ICG 2018: 20th International Conference on Glass** aims to bring together leading academic scientists, researchers and research scholars to exchange and share their experiences and research results on all aspects of Glass. It also provides a premier interdisciplinary platform for researchers, practitioners and educators to present and discuss the most recent innovations, trends, and concerns as well as practical challenges encountered and solutions adopted in the fields of Glass.

Contact: https://www.waset.org/conference/2018/09/prague/ICG